

PAPER • OPEN ACCESS

## Quantum enhanced correlated interferometry for quantum gravity tests: the experimental set-up and the locking scheme

To cite this article: S. T. Pradyumna *et al* 2019 *J. Phys.: Conf. Ser.* **1275** 012020

View the [article online](#) for updates and enhancements.



**IOP | ebooks™**

Bringing together innovative digital publishing with leading authors from the global scientific community.

Start exploring the collection—download the first chapter of every title for free.

# Quantum enhanced correlated interferometry for quantum gravity tests: the experimental set-up and the locking scheme

S.T. Pradyumna<sup>1,2</sup>, E. Losero<sup>1,2</sup>, P. Traina<sup>1</sup>, I. Ruo-Berrchera<sup>1</sup>, I. Degiovanni<sup>1</sup>, M. Zucco<sup>1</sup>, M. Genovese<sup>1,3</sup>

<sup>1</sup>INRIM, Strada delle Cacce 91, 10135, Torino, Italy

<sup>2</sup>DET, Politecnico di Torino, Corso Duca degli Abruzzi 24, 10129, Torino, Italy

<sup>3</sup>INFN, sezione di Torino, via P. Giuria 1, 10125 Torino, Italy

E-mail: m.genovese@inrim.it

**Abstract.** The search for Planck scale effect is one of holy grails of physics. In Fermilab a double Michelson interferometer was built for this purpose: the holometer. In this proceedings we review our effort to build a quantum enhanced holometer.

## 1. Introduction

The search for Planck scale effect is one of holy grails of physics. In Fermilab a double Michelson interferometer was built for this purpose: the holometer [1]. In this proceedings we review our effort to build a quantum enhanced holometer. In particular, we study in detail a system of two power-recycling Michelson interferometers aimed at detecting extremely faint phase fluctuations. This system can represent a breakthrough for detecting a faint correlated signal that would remain otherwise undetectable even using the most sensitive individual interferometric devices. A faint correlated phase noise acting in both the interferometers can emerge, for example, by performing the cross-correlation of their outputs whilst shot noise being uncorrelated in the two interferometers is rejected. Injecting quantum light in the system through the antisymmetric port of each interferometer can further reduce the uncertainty in the measurement of phase correlation. The improvement introduced by quantum light is theoretically discussed in [2, 3], in particular two cases are considered: two single-mode squeezing and twin-beam state. An experiment demonstrating the advantage of using quantum light in a holometer-like set-up has been developed and is at its final stage. This paper describes in details the experimental set-up.

The general idea is represented in Fig. 1



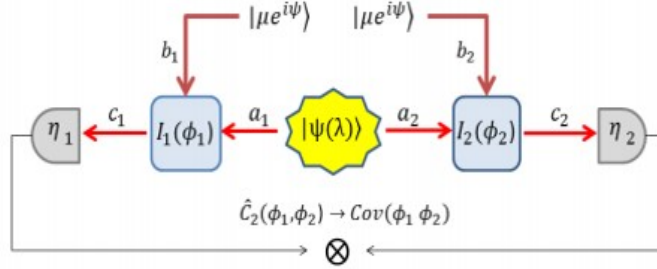


Figure 1: Scheme representing the general idea of a quantum enhanced correlation measurement.  $I_1(\phi_1)$  and  $I_2(\phi_2)$  are two power-recycling Michelson interferometer fed by the coherent state  $|\mu e^{i\psi}\rangle$ . A quantum bi-partite state  $|\Psi(\lambda)\rangle$  can be sent in the interferometers from the classically unused port. From measuring the observable  $\hat{C}(\phi_1, \phi_2)$  the correlation of the two interferometers phases  $\phi_1$  and  $\phi_2$  can be estimated. The use of quantum light can enhance the sensitivity of this measurement. Picture from [2]

Let us consider two Michelson interferometers placed close to each other fed with two coherent states  $|\mu e^{i\phi}\rangle$  in  $b_k$  inputs. The quantum state  $|\Psi\rangle$  (it can be the product of two independent squeezed states or a two-modes twin-beam state) is injected from the antisymmetric ports  $a_1$  and  $a_2$  of the interferometers. The observable  $\hat{C}(\phi_1, \phi_2)$  between the outputs of the interferometer is measured. From  $\hat{C}(\phi_1, \phi_2)$  it is possible to retrieve the correlation in the phases fluctuation, i.e.  $\text{Cov}(\phi_1, \phi_2)$  (see [2, 3] for details). The observable  $\hat{C}$  is different for the two input quantum states considered, in order to minimize the uncertainty on  $\text{Cov}(\phi_1, \phi_2)$ .

### 1.1. Single mode squeezed states

When independent squeezed vacuum states are injected into the interferometer,  $\hat{C}(\phi_1, \phi_2)$  can be chosen as the product of the photon number operators  $\hat{N}_1 \hat{N}_2$ . However to remove the dc component, we evaluate

$$\hat{C}(\phi_1, \phi_2) = (\hat{N}_1 - \langle \hat{N}_1 \rangle)(\hat{N}_2 - \langle \hat{N}_2 \rangle). \quad (1)$$

It can be demonstrated that in ideal situations when losses are zero the uncertainty on the covariance is  $\mathcal{U}^{(0)}(\delta\phi_1 \delta\phi_2) \propto e^{-r_1} e^{-r_2}$ , being  $r_1$  and  $r_2$  the two squeezing factors [2, 3].

### 1.2. Twin-beam state

The second quantum state considered is the twin-beam state: in this case each mode of the twin-beam state is injected into each interferometer. The general operator  $\hat{C}(\phi_1, \phi_2)$ , differently from the case of independent squeezed vacuum, is defined as  $(\hat{N}_1 - \hat{N}_2)^2$ . The results of the theoretical uncertainty reduction in correlated phase detection is thoroughly discussed in [2, 3] It comes out that the uncertainty reduction is divided into two regimes: quadrature correlations regime and photon number entanglement regime. For extremely high detection efficiencies, together with the parameter condition  $T\lambda \gg (1-T)\mu$  the photon number correlation dominates and leads to a dramatic reduction in the uncertainty.  $T = \cos^2(\phi)$  is the interferometer equivalent transmission of the input port (mode)  $a_j$  to the output port (mode)  $c_j$  ( $j=1,2$ ),  $\lambda$  and  $\mu$  are the mean number of photons in the coherent and squeezed mode respectively. While for the opposite condition  $T\lambda \ll (1-T)\mu$  and slightly away from dark fringe, twin-beam quadrature correlations can be exploited and the uncertainty behaves similarly to the independent squeezed

states case. Twin-beam state can be generated by superimposing two single mode squeezed states at a BS, however a twin-beam-like state which has the same non-classical behavior, in terms of quadratures correlation (although only in one quadrature angle), can be generated by splitting a single mode squeezer on a 50-50 beam splitter. This simpler option is implemented in the experiment.

## 2. Classical part: power-recycling MI

Our system consists of two power-recycling Michelson interferometers placed close to each other with small separation between the two beam-splitters.

These are the types of interferometer currently operated at larger scale gravitational-wave detectors. They are based on the combination of two fundamental interferometers : the Fabry-Perot interferometer and the Michelson interferometer.

A Fabry-Perot cavity is a linear cavity formed by two partially reflecting mirrors. When light is incident on this linear cavity, some part is transmitted and some part is reflected. The beam is transmitted through the cavity only when the length of the cavity  $L$  matches the multiple of wavelength  $\lambda$  of the light incident. In correspondence, the optical power inside the cavity is enhanced (optical gain) because of constructive interference of repeated reflections. The transmission in the cavity is maximum when  $2kL$  is multiple of  $2\pi$  which implies (whenever the detuning frequency  $\nu$  is a multiple of  $c/2L$ ) the transmission of the cavity is maximum. This spacing of the detuning between two successive maxima or two successive minima of the transmission (and/or optical gain occurrence) of the cavity  $\Delta\nu = c/2L$  is called Free Spectral Range (FSR). Another property, which defines the losses in the cavity, is the finesse. It is defined as the ratio of Free Spectral Range of the cavity to the Full-Width-at-Half-Maximum (FWHM) of the transmitted peak. It defines the quality of the cavity. In general, the optical losses of the cavity widen the peak, decreasing the value of the finesse.

A Michelson interferometer consists of a 50-50 beam splitter and two piezo transducer driven end-mirrors. The laser field entering from the input port propagates in each arm of the interferometer, before reflecting back towards the beamsplitter. The two beams interfere at the beam splitter: the intensity of the transmission and reflection depends on the differential arm length (DARM) ( $L - L'$ ) and can be sensed by measuring the power at the anti-symmetric port, using a photodetector. The DARM point corresponding to constructive interference at the anti-symmetric port is called bright fringe while the one corresponding to destructive interference is called dark fringe.

The figure of merit to quantify the contrast between the dark and bright fringe is the interferometric visibility and is given by:

$$V = \frac{(P_{max} - P_{min})}{(P_{max} + P_{min})} \quad (2)$$

When a Michelson interferometer is operated near the dark fringe, most of the power is reflected back towards the laser. This reflected power could be recycled by placing a partially transmitting mirror called power-recycling mirror (PRM) and forming a resonant cavity with the interferometer. In this sense the power-recycling interferometer is combination of a Fabry-Perot cavity and Michelson interferometer. With this technique, as the optical power  $P$  in the interferometer is increased by the power-recycling, the shot noise reduces as the uncertainty is proportional to  $(P)^{-1/2}$ . The Michelson interferometer operated at the dark fringe can be considered as a high-reflective compound mirror. The recycling mirror forms a recycling cavity with this compound mirror of equivalent length  $CARM = \frac{L+L'}{2}$ ; the power in the cavity is enhanced when the cavity is resonant with the input laser beam.

Fig. 2 depicts the simplified schematic of our experimental setup, concerning the classical part.

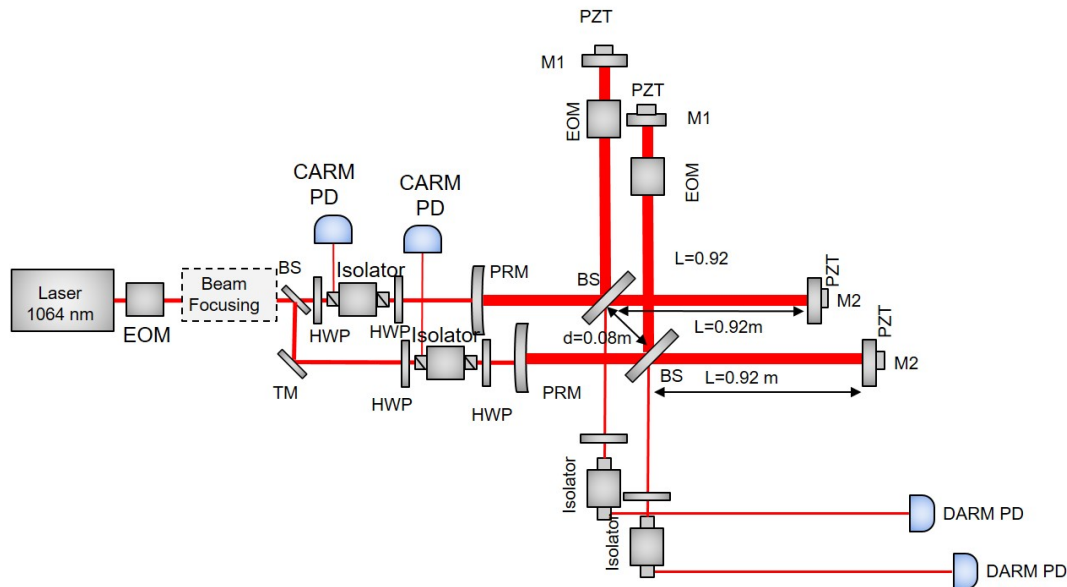


Figure 2: Simplified schematic of the double-interferometer setup. Two Michelson Interferometers with arm length  $L = 0.92m$  were co-located, with a distance between the two balanced beam splitters (BSs) of around 8cm.  $M_1, M_2$ : piezo-actuated high-reflectivity (99.9%) end-mirrors. PRM: partially reflecting (90%) power-recycling mirror, radius of curvature  $r_c = 1.5m$ .; HWP: Half waveplate; PD: Photodetector; BS: Beam splitter

A Nd-YAG laser with an output power of 300 mW at wavelength 1064nm is used. Part of the light is sent to the generation of the squeezed light setup. For having an efficient TEM00 input mode for the interferometers, the light is fiber coupled. A power of 1.5 mW enters each interferometer.

Each interferometer is formed by a power-recycling mirror having the radius of curvature of 1.5m, a 50-50 beam splitter, and two plain end-mirrors  $M_1$  and  $M_2$  (reflectivity around 99.9%).  $M_1$  and  $M_2$  are stabilized by a PZT actuators. The power-recycling mirror's reflectivity is chosen to be of 90 % to form an over-coupled cavity with end-mirrors when locked near the dark fringe.

The length of each arm of the interferometer is  $\sim 92$  cm. The distance between the two beam splitters is  $\sim 8$  cm. A set of lenses is placed before the interferometers for mode matching the power-recycling interferometer such that the waist of the beam is at the end-mirror. A resonant Electro Optic Modulator (EOM) is placed before the interferometers for generating the proper error signal for locking the CARM (see next section) while another phase modulator, which consists of RTP crystal (4mm x 5mm area) is placed inside the interferometer for locking the DARM. A photodetector with quantum Efficiency 99% is placed at the output port: it is used both for locking the DARM and acquiring the data. Another photodetector, used for locking the CARM, collect the light reflected from the power-recycling cavity.

### 2.1. Locking schemes

Fig. 3 depicts the detailed locking scheme of each interferometer. It is necessary to lock the system to the proper working point, in order to get rid of environmental noise and reach the desired sensitivity. In particular we work close to the dark fringe and at the resonance. The first condition implies for the DARM:  $L - L' = n\lambda + \delta$  while the second condition: CARM  $L_{eff} = \frac{L+L'}{2} = m\lambda$ .

To lock the cavity to the resonance, the Pound-Drever-Hall locking technique is utilized [4]. For this technique it is necessary to induce a periodic phase modulation of the laser beam, applying a periodic electronic signal with a EOM ( $\omega_C = 20\text{MHz}$ ). In this way two fields, called sidebands, separated in frequency from the original field by the modulation frequency are generated. The signal reflected from the cavity is collected by the CARM photodiode, demodulated at  $\omega_C$  and opportunely processed in the lockbox. We have used a set of lock boxes made of Proportional-Integral controller with inbuilt low pass filters) to generate an error signal. This error signal is then sent equally (phase concordance) to both the end-mirrors passing through a high voltage amplifier (HVA).

For locking the DARM at a desired working point different techniques are possible. In our case, being interested in locking close to the dark fringe the internal modulation technique is chosen. As in the PDH technique the generation of sidebands is necessary. In this case the EOM is placed inside the interferometer to generate sidebands at a frequency  $\omega_D = 7.6\text{MHz}$ . The DARM photodiode signal is demodulated by a mixer at the frequency  $\omega_D$  and then sent to the lockbox. The dark fringe corresponds to the zero of the error signal and corresponds to its maximum slope. This error signal is then sent differentially (i.e with a relative phase of  $\pi$ ) to both the mirrors with a help of a High Voltage Amplifier. The phase between the electronic local oscillator (LO) and the AC output signal from the photodetector has to be adjusted properly to maximize the slope of the error signal. Sending the error signal equally for the CARM locking and differentially for the DARM locking allows to decouple the control of the two degree of freedom, i.e. the DARM error signal does not affect the CARM and viceversa.

The locking for the squeezed beam is described in the next section.

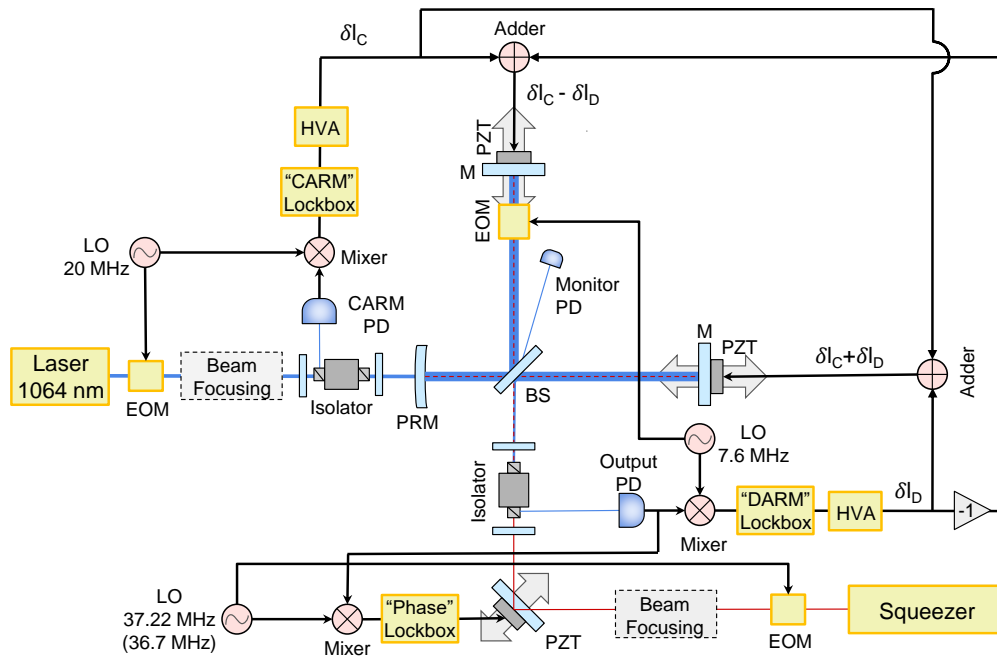


Figure 3: Detailed locking schematic of each interferometer. PZT: piezo-electric actuator. EOM: electro-optical modulator. HVA: high-voltage amplifier. LO: local oscillator. PD: photo-diode, InGaAs with high quantum-efficiency photodiodes (99%) and low noise (Noise Equivalent Power  $1.2 \cdot 10^{-11} \text{W}/\sqrt{\text{Hz}}$ ) are used at the read-out port. Beam-Focusing: set of lenses in order to have Gaussian Optical mode  $\text{TEM}_{00}$ .  $\delta l_C, \delta l_D$ : correction signals from the CARM and DARM lockbox respectively. The DARM was locked using the internal modulation technique while the CARM was locked using the Pound-Drever-Hall technique

### 3. Squeezing generation set-up

Fig. 4 depicts, on the left-hand side, the experimental scheme for preparation of squeezed vacuum state, on the right-hand side, the two quantum states considered and their implementation. In both cases the squeezed light is injected into the interferometers through the anti-symmetric port.

Each squeezer comprises of a ppKTP (periodically poled Potassium Titanyl Phosphate) crystal placed inside a semi-monolithic cavity formed by the edges of the crystal and transparent mirror. A separate 1064nm beam dubbed control beam was sent through a phase modulation of 37.22 MHz and 36.5 MHz respectively for each squeezer cavity and is used to lock each of the squeezer cavities using Pound-Drever-Hall technique. An internal module for second harmonic generation provided the 532 nm radiation as a pump for the generation of squeezed light. The pump beam is then sent to a mode-cleaner to have clean TEM00 mode. The output of the mode cleaner is then incident on the crystal for having parametric down conversion inside the cavity. A Peltier element and a thermistor attached to the crystal was used along with a temperature controller for having an efficient phasematching between the control beam and incoming pump beam. The phase relation between pump and control beam determines the orientation of the squeezing ellipse. A PZT attached to mirror is used to lock this phase. The control beam perfectly overlaps spatially to the generated squeezed light at 1064nm. Thus it is used to align the squeezed light into the interferometer and to adjust the spatial mode matching between the beam in the interferometer cavity and the squeezed beam. A dichroic beam splitter (DBS) is used to reflect the 1064 nm and would not allow any 532 nm to be injected into the interferometer. Since squeezer is very sensitive to loss, a very high reflective turning mirrors ( $R \sim 99\%$ ) were used to inject into interferometers.

The squeezed light after it passes through DBS is injected into the interferometer, previously locked near to the dark fringe. The control beam, with output power maintained at  $5\mu\text{W}$ , enters the interferometer together with the squeezed light. When the squeezed light enters the interferometer, the DARM photodetector is demodulated at 37.22 MHz/36.5 MHz with an inbuilt mixer. The error signal is generated such that the point of squeezing quadrature corresponds to the maximum slope part of the error signal. The interferometer is then locked to the squeezing quadrature by help of a phase shifter with PZT attached.

The TEM 00 interferometer output mode has to be modematched to the squeezed light. This is done by reversing the injection of interferometer mode into the squeezer cavity. Appropriate lenses are placed to improve the mode-matching between the interferometer output mode and squeezed light mode. The squeezer cavity which has a PZT attached to it is scanned and modes of the cavity are observed. The TEM 00 mode was enhanced by turning mirrors placed for aligning the squeezed light to the interferometer. At the end of the procedure the modematching was around 99%.

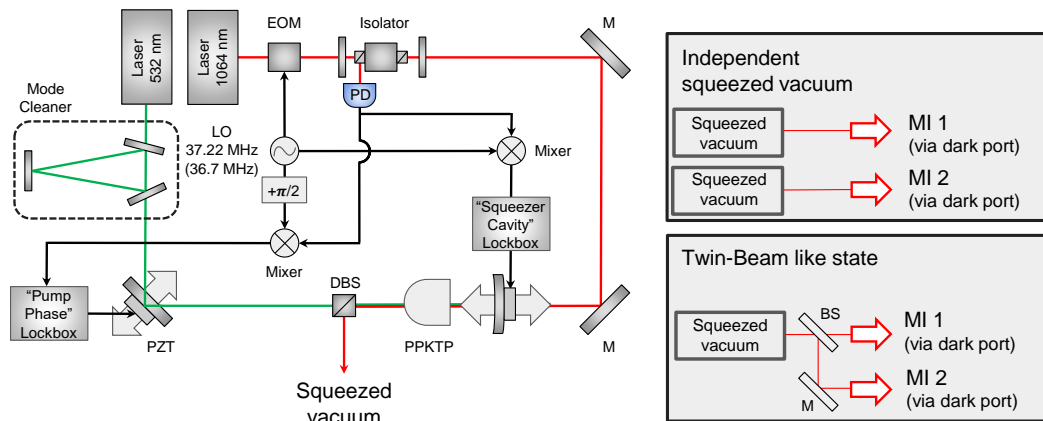


Figure 4: On the left-hand side a scheme of the squeezer generation set-up is presented, see text for the details. On the right-hand side the quantum states tested are summarized: independent single mode squeezed vacuum and twin-beam like state.

The twin-beam state is entangled in number of photons and presents also non classical quadrature correlations between the two optical modes. Although photon number entanglement would provide in principle a dramatic enhancement of the sensitivity, its practical realization is extremely challenging. On the other side exploiting non-classical quadrature correlations is definitely feasible with some slight modification of the previous configuration.

As anticipated in the introduction we use an approximate twin-beam-like state in our experiment. Its implementation is straight forward having implemented the two single mode squeezing configuration. The quantum noise locking is similar to that of the double squeezer setup previously described, in this case the sidebands are both at 36.5 MHz in the two modes. The main difference respect the two single-mode squeezed beams is in the data elaboration: the variance of difference of the output signal of two interferometers is considered instead that the correlation.

## References

- [1] Chou AS, Gustafson R, Hogan C, Kamai B, Kwon O, Lanza R, McCuller L, Meyer SS, Richardson J, Stoughton C and Tomlin R 2016 First measurements of high frequency cross-spectra from a pair of large Michelson interferometers. *Physical Review Letters* **117** 111102
- [2] Ruo-Berchera I, Degiovanni IP, Olivares S, Samantaray N, Traina P and Genovese M 2015 One-and two-mode squeezed light in correlated interferometry. *Physical Review A* **92** 5 053821
- [3] Ruo-Berchera I, Degiovanni IP, Olivares S and Genovese M 2013 Quantum light in coupled interferometers for quantum gravity tests. *Physical Review Letters* **110** 21 213601
- [4] Black ED 2001 An introduction to Pound–Drever–Hall laser frequency stabilization. *American Journal of Physics* **69** 1 79-87